FINITE ELEMENT STUDY OF ELASTIC WAVE INTERACTION WITH CRACKS

Z. You and W. Lord

Department of Electrical Engineering
and Computer Engineering
Iowa State University
Ames, Iowa 50011

INTRODUCTION

Ultrasonic means have been used for the nondestructive evaluation (NDE) of a wide variety of mechanical properties in solid materials. Defects such as cracks and inclusions act as sources of wave scattering when illuminated by an incident pulse through reflection, diffraction and mode conversion. Interaction of elastic waves with cracks provides all the needed information relative to inverse characterization of the defects which has not been thoroughly solved yet. Fully understanding these interactions will provide more knowledge for implementing inverse algorithms.

Analytical work has been carried out for studying particular scattering situations [2-4]. Mode conversions are emphasized by many authors and Bond [5] defines a "total-wave technique" which is intended to extract more of the information available in ultrasonic wave fields. The interaction is complex, for example, when Rayleigh pulses are used to probe surface breaking slots in metal, some elastic mode conversion takes place in the region of the slot. A proportion of the Rayleigh pulse is converted into shear mode, which may then be reflected along the surface, scattered into the bulk of the material, or transmitted beyond the slot. In the case of a longitudinal incident wave, a shear wave can also show up because of the mode conversion taking place on the surface of the cracks. At the same time, edge waves are produced at the tips of the crack. Experiments using laser generated ultrasound [1] prove some of these phenomena. Mostly, however, the analytical approaches are restricted to infinite or semi-infinite space, and the interactions of scattered waves from two or more defects are neglected. Also, general anisotropy and realistic transducer and defect shapes are very difficult to take into account in analytical approaches.

Because of their ability to simulate realistic engineering problems, numerical techniques are particularly applicable to NDE fields where energy/defect interactions are of considerable importance. It can be said that only numerical approaches naturally combine all the coupled wave phenomena together in one situation with complicated geometries. Finite difference techniques [6,7] also show promise in modeling the coupled wave phenomena in regular geometries. The finite element method is superior in that it is easier to deal with the awkward geometries such as complex shaped defects associated with NDE. Previous papers [8-10] have reported on the development of finite element modeling to elastic wave propagation in elastic media. The applications are restricted to small geometries. This paper emphasizes the wave/defect interactions, and both space and time discretization problems are discussed.

FINITE ELEMENT FORMULATION

By applying Hooke's law, the general equation of motion in elastic media can be written in terms of the displacement vector as

$$C_{ijkl}\, u_{k,lj} = \rho \ddot{u}_i \tag{1}$$

where C_{ijkl} is the tensor elastic constant, ρ is the material density, and the subscripts i, j, k, l can be x, y, or z.

The finite element solution of this hyperbolic equation includes the discretization of the region into a series of simple elements, the approximation of the field values interior to the element in terms of its nodal values through the shape function, and the determination of the nodal values through the minimization of the energy functional

$$F = \int_v u_{i,j} T_{ij}\, dv - \int_s u_i t_i\, ds + \int_v u_i \rho \ddot{u}_i\, dv \tag{2}$$

where the second term is the work done by the surface traction t_i, the third term is body kinetic energy, and the first term represents the body potential energy where T_{ij} is the stress tensor defined as

$$T_{ij} = C_{ijkl} S_{kl} \tag{3}$$

where the strain tensor

$$S_{kl} = \frac{1}{2}\left(u_{k,l} + u_{l,k}\right) \tag{4}$$

The final form of the finite element formulation results in the following ordinary differential equation

$$KU_t + M\ddot{U}_t = F_t \tag{5}$$

where K and M are the global stiffness and mass matrices respectively. They are the direct results of assembling all element matrices K^e and M^e, which are a function of element geometry and material parameters.

Equation (5) may be solved by a variety of methods. We will here restrict our attention to an explicit central difference formula

$$\ddot{U}_t = \frac{1}{\Delta t^2}\left(U_{t+\Delta t} - 2U_t + U_{t-\Delta t}\right) \tag{6}$$

Inserting (4) to (3) yields

$$\frac{1}{\Delta t^2} MU_t = F_{t-\Delta t} - \left(K - \frac{2}{\Delta t^2} M\right) U_{t-\Delta t} - \frac{1}{\Delta t^2} MU_{t-2\Delta t} \tag{7}$$

The mass matrix is not diagonal, which often results in a considerable increase of computational expense because the inverse of M is required for solving U_t from equation (7). As an approximation, the mass matrix can be diagonalized as its diagonal terms multiplied by a scaling factor, that is

$$M_{ij}^{diag} = \begin{cases} \alpha\ M_{ij}, & \text{if } i = j \\ 0, & \text{if } i \neq j \end{cases} \tag{8}$$

where

$$\alpha = \frac{\sum_i \sum_j M_{ij}}{\sum_i M_{ii}} \tag{9}$$

The equation (7) now becomes an iteration formula for U_t from $U_{t-\Delta t}$ and $U_{t-2\Delta t}$. The iteration can be started with initial conditions

$$U_0 = 0$$
$$U_{-\Delta t} = 0$$

which implies that the system is in a zero state before time zero.

Even though most texts mention that the explicit formula (6) requires smaller time discretization because of poor accuracy and instability in comparing with the implicit integration scheme, this is not necessarily true for our ultrasonic wave predictions. Because of the high frequency, the restriction on the spatial discretization is very crucial, the time step size required by the spatial step size is much smaller than that required by the algorithm itself. More details are given in the next section.

One direct result of using the explicit formula is the increase of efficiency which includes both memory and CPU time. Large size geometries can be handled only by using this scheme.

DISCRETIZATION CONSIDERATIONS

Discretization is an important factor in considering both accuracy of results and computational expense. A major objective of the following mesh study is to find out the appropriate level of discretization necessary to obtain correct results. Both space and time discretization for realistic results are considered.

A 10cm x 5cm aluminum block excited by a line source at the center is chosen to study the spatial discretization problem. Only one-half of the block is discretized because of the symmetrical condition along the centerline. Three typical results are shown in Fig. 1, which tells us that at least eight nodes per shortest wavelength are required in order to produce all the artifacts (head, surface, longitudinal and shear waves) associated with such a situation. If more accurate results are required which possess better consistency of the waveform, twelve nodes per shortest wavelength are recommended. Sixteen nodes per shear wavelength were used for computing the A-scan data in comparisons with corresponding analytical results.

The time step size should be chosen such that the wave travels less than the spatial step size in one time step. The study shows that the time step required for stability and accuracy of the algorithm itself is automatically satisfied under the above condition.

RESULTS

Several examples are studied by using the finite element method. The first one is a 20cm x 10cm aluminum block with a rectangular slot of dimension 8mm x 0.4mm in the center. The geometry is shown in Fig. 2. The line source applied is a triple cosine waveform

$$f(t) = \left(1-\cos\frac{\omega_0 t}{3}\right)\cos\omega_0 t \qquad (10)$$

where

$$\omega_0 = 2\pi f$$
$$F = 1MHz$$

Because of the symmetry, only one-half of the geometry is discretized into 250 x 250 = 62500 rectangular elements. The wavefronts at particular time steps are plotted in Fig. 3. From these plots, it should be observed that the longitudinal, shear, surface, and head waves are all started from the same line source, and separated as they travel further into the material because of the different traveling velocity. At about 10ns, the longitudinal wave arrives at the slot and forms a strong reflection which can be detected on the surface. The main L-wave is distorted and acts as the transmission part which can be used in inverse algorithms. More interesting phenomenon may be the two rings traveling with shear velocity formed through the mode conversion of the L-wave/defect interaction at the tips.

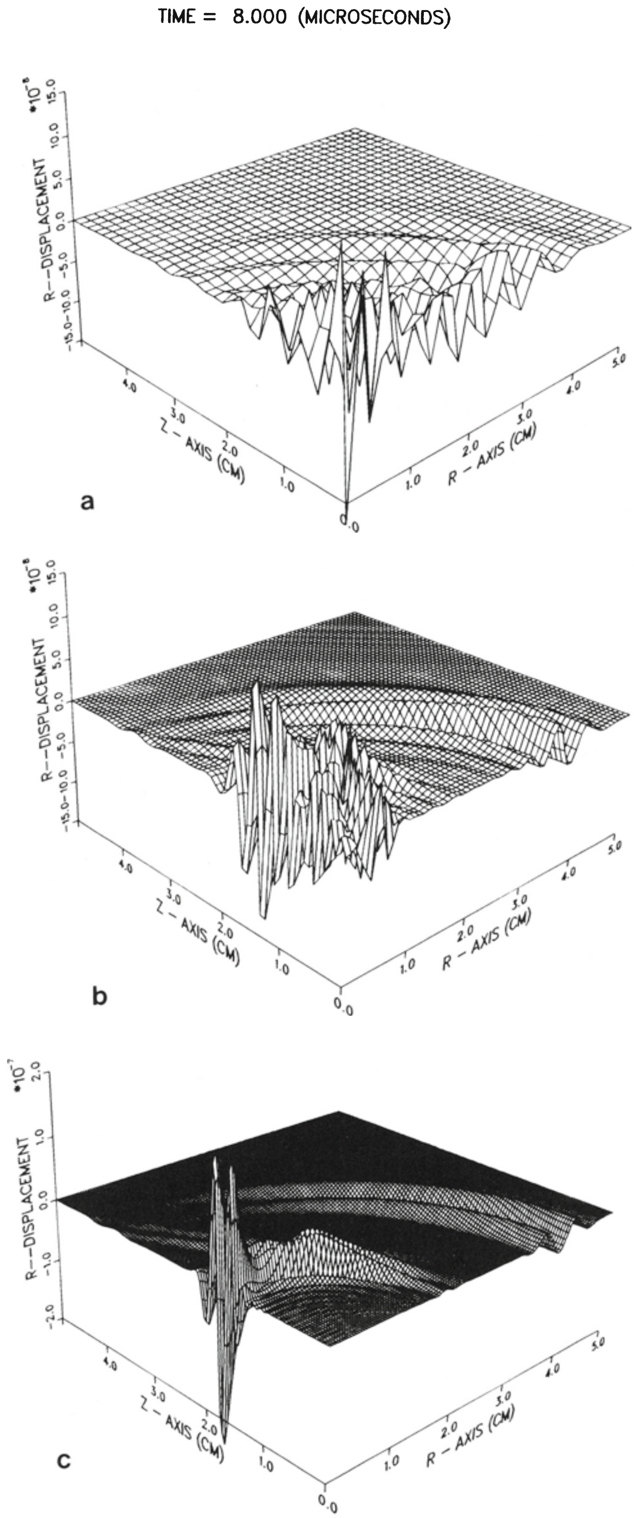

Figure 1. Wavefront comparisons at different discretization levels: a) 2 nodes per shear wavelength; b) 4 nodes per shear wavelength; c) 8 nodes per shear wavelength.

Fig. 3 may also remind us of the fact that a line source launches a strong surface wave which can be used to study the surface wave phenomena as in the following example shown in Fig. 4. The two surface breaking cracks are located symmetrically with respect to the y-axis. As a result of this choice, the symmetrical condition can still be applied at the centerline. The displacement plots are shown in Fig. 5. For the purpose of showing more detail around the crack, only one quarter of the geometry is plotted. It can be seen that a fairly strong reflection is formed at the first corner. At the tip, the main portion of the transmitted wave from the first corner is converted to the shear wave which travels into the material. Only a very small part of the incident surface wave is transmitted beyond the crack.

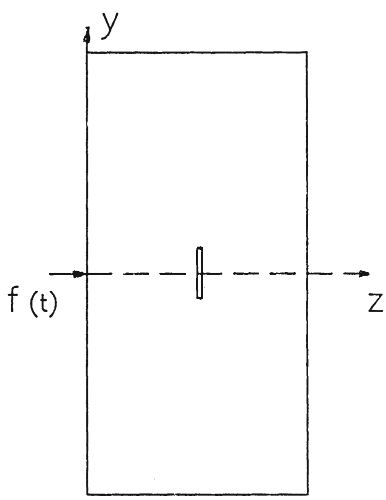

Figure 2. Geometry detail of the example used for studying L-wave/defect interactions.

CONCLUSIONS

The explicit integration scheme discussed in this paper now allows the developed 2-D finite element code to handle reasonable sized blocks in fine mesh. Both space and time discretizations are important and should be carefully chosen in numerical modeling studies. Interactions of elastic waves with cracks are illustrated with the 2-D displacement plots, and all the results confirm the validity of finite element modeling.

ACKNOWLEDGEMENT

This research has been supported by the Electric Power Research Institute and the Computer Center of Colorado State University.

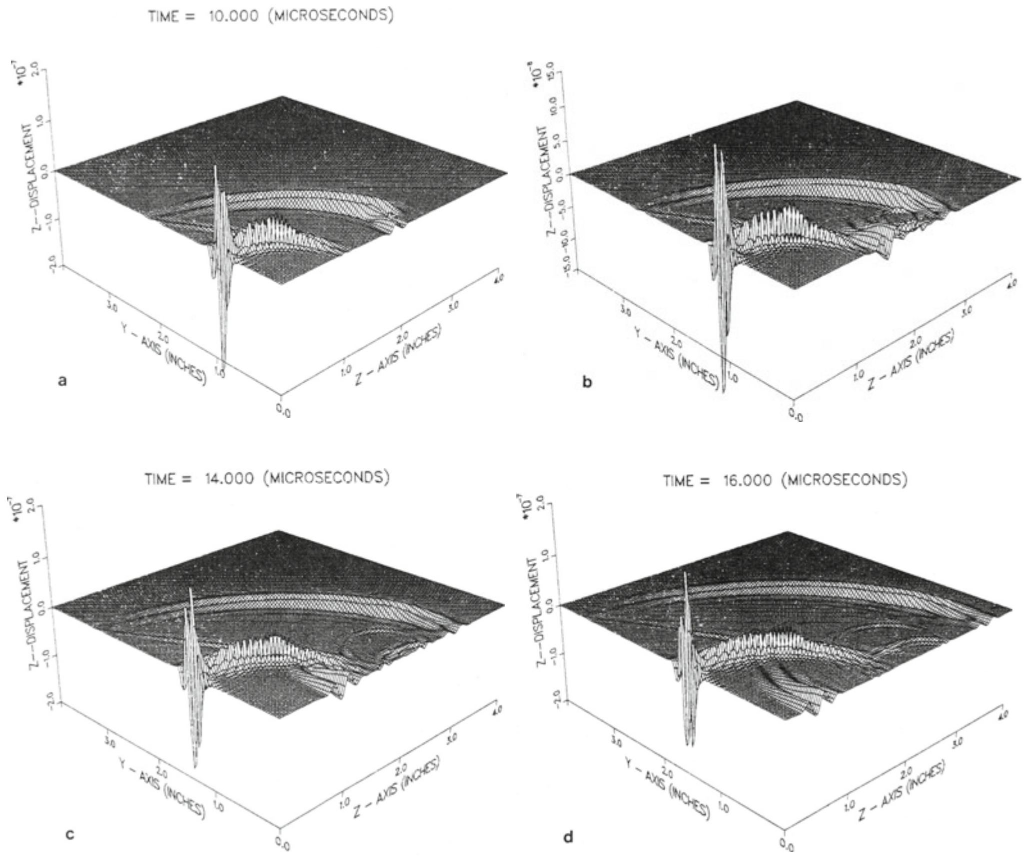

Figure 3. Displacement plots of the L-wave/defect interactions.

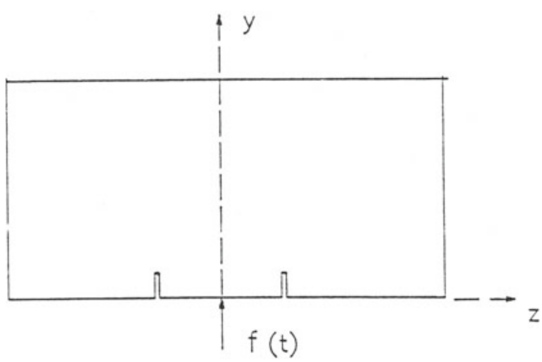

Figure 4. Geometry detail of the example used for studying surface wave interaction with cracks.

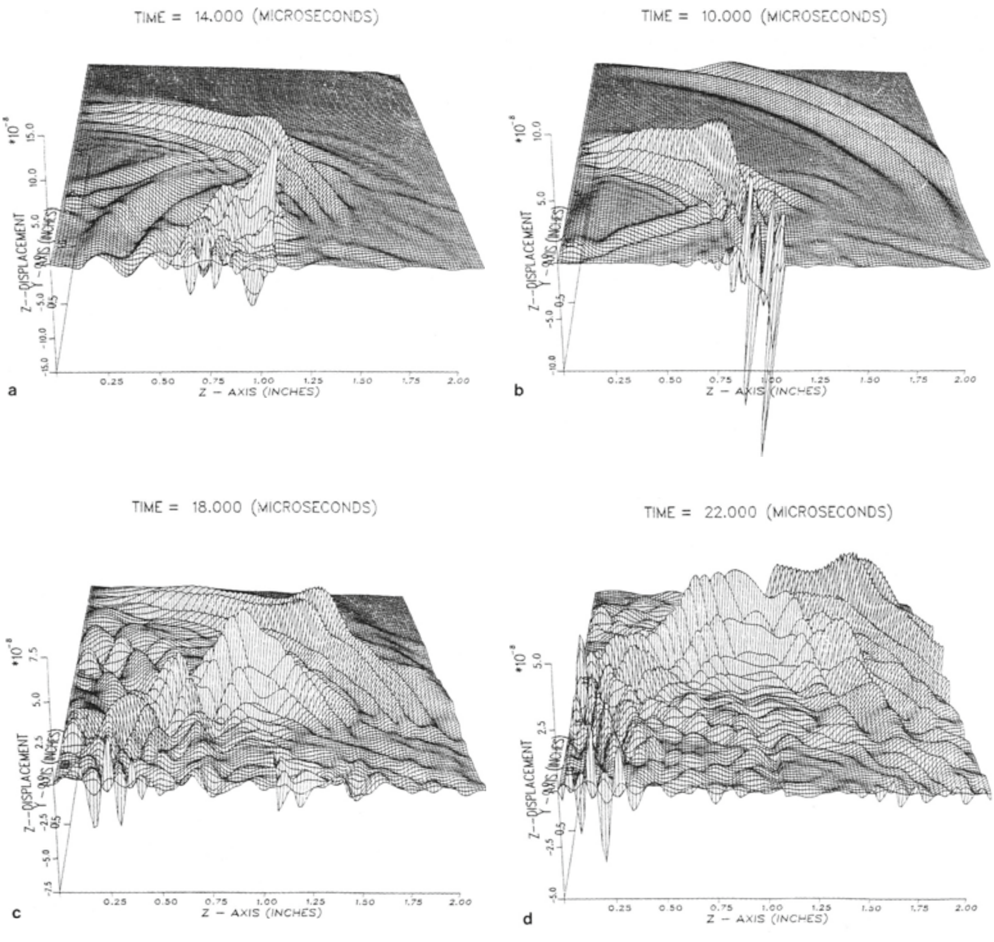

Figure 5. Displacement plots of the surface interaction with a crack.

REFERENCES

1. J. A. Cooper, eta., "Surface Acoustical Wave Interaction With Cracks and Slots: A Noncontacting Study Using Lasers", IEEE Trans. on UFFC, vol. UFFC-33 , No. 5, pp. 462, 1986.
2. C. F. Ying, and R. Truell, "Scattering of a Plane Longitudinal Wave by a Spherical Obstacle in an Isotropically Elastic Solid", J. Appl. Physics, vol. 27 , pp. 1086, 1956.
3. J. D. Achenbach, eta., "Scattering from Surface-Breaking and Near-Surface Cracks", Wave Propagation in Homogeneous Media and Ultrasonic Nondestructive Evaluation , 1984.
4. R. K. Chapman and J. M. Coffey, "A Theoretical Model of Ultrasonic Examination of Smooth Flat Cracks", Review of Progress in Quantitative NDE , vol. 3A, pp. 151, 1984.
5. L. J. Bond and N. Saffari, "Mode Conversion Ultrasonic Testing", Research Techniques in Nondestructive Testing , vol. 7, pp. 145, 1984.
6. L. J. Bond, eta., "Modeling Ultrasonic Waves Using Finite Difference Methods", ibid. pp. 135.
7. K. Harumi, "Computer Simulation of Ultrasonics in a Solid," Material Evaluation, vol. 44, pp. 1086, 1986.
8. R. Ludwig and W. Lord, "A Finite Element Formulation for Ultrasonic NDT Modeling", Review of Progress in Quantitative NDE , vol. 4A, pp. 37, 1985.
9. R. Ludwig and W. Lord, "Developments in the Finite Element Modeling of Ultrasonic NDT Phenomena", Review of Progress in Quantitative NDE , vol. 5A, pp. 73, 1986.
10. Z. You, W. Lord, and R. Ludwig, "Numerical Modeling of Elastic Wave Propagation in Anisotropic Materials", Review of Progress in Quantitative NDE , vol. 7A, pp. 23, 1988.